

Article

Development and Characterization of Electrospun Nanostructures Using Polyethylene Oxide: Potential Means for Incorporation of Bioactive Compounds

Sergiana dos P. Ramos ¹, Michele A. Giaconia ¹, Jonas T. Do Marco ¹, Robert da S. Paiva ², Veridiana V. De Rosso ¹, Ailton C. Lemes ³, Mariana B. Egea ⁴ , Marcelo Assis ², Tatiana M. Mazzo ⁵, Elson Longo ² and Anna R. C. Braga ^{1,6,*}

¹ Department of Biosciences, Universidade Federal de São Paulo (UNIFESP), Silva Jardim Street, 136, Vila Mathias, Santos 11015-020 SP, Brazil; sergiana.ramos@gmail.com (S.d.P.R.); michelegiaconia@hotmail.com (M.A.G.); jonasthmarco@gmail.com (J.T.D.M.); veridiana.rosso@unifesp.br (V.V.D.R.)

² Chemistry Department, CDMF/LIEC (UFSCar), P.O. Box 676, São Carlos 13560-970 SP, Brazil; robert21sp@gmail.com (R.d.S.P.); marcelostassis@gmail.com (M.A.); elson.liec@gmail.com (E.L.)

³ Department of Biochemical Engineering, Universidade Federal do Rio de Janeiro (UFRJ), Technological Center, School of Chemistry, Ilha do Fundão, Av. Athos da Silveira Ramos, 149, Rio de Janeiro 21941-909, Brazil; ailtonlemes@eq.ufrj.br

⁴ Federal Institute of Education, Science and Technology Goiano, Campus Rio Verde, Rio Verde 75901-970, Brazil; mariana.egea@ifgoiano.edu.br

⁵ Institute of Marine Sciences, Universidade Federal de São Paulo (UNIFESP), P.O. Box 11070-100, Santos 11015-020 SP, Brazil; tatimazzo@gmail.com

⁶ Department of Chemical Engineering, Universidade Federal de São Paulo (UNIFESP), Campus Diadema, Diadema, São Paulo 09972-270, Brazil

* Correspondence: anna.braga@unifesp.br; Tel.: +55-13-981450201

Received: 19 March 2020; Accepted: 13 April 2020; Published: 17 April 2020



Abstract: The development of processes for stabilization of the properties of bioactive compounds has been studied in recent years, and the use of nanotechnology is among the most discussed routes. The present work addressed the assembly of nanostructures using polyethylene oxide (PEO), the production of core-shell nanofibers (NFs) with bioactive compounds, and the evaluation of their microscopic and physical characteristics. Aqueous solutions of PEO were electrospun by varying different process and solution parameters (PEO and NaCl concentrations, feeding rate, the tip-to-collector distance (TCD), and applied voltage) in order to optimize production of nanostructures. The best condition obtained was evaluated to form core-shell NFs composed by jussara pulp as a source of anthocyanins. To assess the production of NFs with PEO and jussara pulp, feed solutions were prepared in acetate buffer (pH 4.5) with 6% PEO and 10% lyophilized jussara pulp, at a feeding rate of 150 $\mu\text{L}\cdot\text{h}^{-1}$ and TCD of 15 cm using an applied voltage of 10 kV to form core-shell NFs. The results revealed the formation of core-shell NFs with a diameter of 126.5 ± 50.0 nm. The outcomes achieved represent a crucial step in the application of anthocyanins in food systems as pigments, establishing a basis for further research on the incorporation of nanomaterials into foodstuff.

Keywords: electrospinning; nanofibers; encapsulation; bioactive compounds

1. Introduction

Electrospinning is a method that was developed in the early 20th century, and it is known to be a versatile and economical fiber formation technique that is suitable for the production of

nanometer-sized fibers. In recent years, this method has improved significantly in terms of instrument design and, moreover, by the possibility of extruding a wide range of polymers [1,2].

Electrospinning involves the drawing of fluid in the form of either molten polymer or polymer solution and, unlike conventional drawing methods where an external mechanical force pushes the molten polymer through a die, electrospinning makes use of charges that are applied to the fluid, causing a stretching force to be applied to a collector in which there is a potential gradient. When a sufficiently high voltage is applied, a jet of polymer solution will erupt from a droplet of the mixture. The electrospinning of polymer solutions relies on the evaporation of the solvent, which allows the polymer to solidify, thus forming polymer fiber. This technique has been employed to produce continuous fibers from a wide variety of materials—including nanofibers (NFs) possessing diameters of a few nanometers—and the process, therefore, offers exceptional flexibility [3,4].

During the electrospinning process, if the compound of interest and the carrier material are mixed and erupt from a droplet of the solution through the application of the electrical field using a single tip, then the manner in which the electrospun structure is obtained is referred to as being uniaxial. On the other hand, in the coaxial electrospinning mode of operation, two concentric capillaries are used to expel polymer solution and the compound simultaneously from two different needles [5,6].

With respect to the polymers applied, polyethylene oxide (PEO) is a water-soluble synthetic polymer that has been designated Generally Recognized as Safe (GRAS) by the Food and Drug Administration (FDA). Hence, it can be quickly and safely used in processed food and beverages [7]. The preparation of polymeric solutions through the addition of salt, such as NaCl, is a common technique used in the manufacturing of NFs through the electrospinning process. The addition of NaCl increases the number of ions introduced to the solution. Thus, additional elongation forces are imposed to the jet under the electrical field, leading to the production of more uniform NFs with smaller diameters [8,9].

Electrospun fibers can be electrostatically charged, and the charge can be manipulated, removed by exposure to ions carried in the air or neutralized through contact with the collector. If the fibers are electrically conductive, the charge can also be adjusted by conduction through the fiber. Polymers such as PEO, polycaprolactone (a polyester), polycarbonate, and polystyrene have been evaluated for their charge induction and charge retention characteristics, and ranked with respect to their inherent polarity. PEO has been shown to possess great versatility and diverse applicability, while also demonstrating ease of manipulation in order to obtain structures in a nanosized scale [5,10–12].

The stability of bioactive compounds may be affected by several factors, including the nature of the pigment, light, temperature, pH, metal ions, enzymes, oxygen, and antioxidant agents [13]. Furthermore, some operational parameters are critical in the context of large-scale application of bioactive compounds in foodstuff.

However, the use of natural pigments and additives in processed foods and beverages is essential for increasing consumer acceptability of these products, especially since these pigments are natural colorants with low to no toxicity. It has been established that natural pigments are safer for consumption—even at higher doses than synthetic dyes [14,15]. Consequently, a number of studies have been carried out searching for means to employ these compounds while minimizing their unfavorable effects. With respect to the release of bioactive compounds, it is necessary to consider their practical applications [16,17]. Indeed, in systems where the biocomposite must act as a preservative or even a pigment, a gradual release is required in order to preserve the food matrix during storage. On the other hand, in cases where the nanostructured biocomposite is intended to have an impact on health, its release must take place after being ingested and passed through the gastrointestinal tract, as its bioactivity will be relevant only once the material has been systemically absorbed [15,18,19].

In this sense, the development of technologies and processes for the stabilization of certain features of bioactive compounds has been studied in the recent years, and nanotechnology is currently among the most discussed methods [20–22]. Nevertheless, nanostructured forms of bioactive compounds that could enable the stabilization of natural pigments, such as NFs, have not been widely evaluated.

In this sense, electrospinning can be considered an excellent technique for the formation of bioactive compounds carriers since the process occurs in a closed working system, which allows for a faster, secure and efficient production. Most of all, the procedure does not require specific solutions and can be executed under ambient temperature [2]. Although the electrospinning technique has already been applied to obtain nanostructures using PEO as the basis [22–25], none of the consulted manuscripts have simultaneously evaluated the main parameters of the electrospinning process. Hence, we hypothesized that variations in process settings allied to changes in polymer and NaCl concentrations will affect the resulting material in terms of structure, form, and size.

Among the bioactive compounds constituting fruits and vegetables, anthocyanins are particularly remarkable, due to their potential industrial application as natural pigments. Likewise, this bioactive compound has shown several positive effects over human health, as numerous studies reported in the latest years [19,26,27]. The main property described regards their antioxidant capacity, since this pigment acts as free radical scavengers, which is frequently linked to the prevention of chronic diseases [28,29]. The fruit of *Euterpe edulis* Mart., commonly called jussara, presents high contents of anthocyanins and is very similar to the açai berry in both its sensorial and nutritional properties. Jussara has been extensively considered as a superfruit and highlights the potentialities related to the Brazilian biodiversity as a source of high-value products. Studies in our group showed that jussara, besides the colorant power provided by the anthocyanins, is accounted for in several beneficial results from a perspective of health and well-being [27,30–32]. Jussara pulp has been recognized as a superfood due to its composition, mainly, for the high concentration of anthocyanins and other phenolic compounds; in fact, these bioactive compounds are considered an attractive source of pigments and also means to ward off several diseases [27,33,34]. In this context, the pulp as a whole can be used in food preparations to confer color and beneficial biological effects.

Biomolecules present in fruits and other sources are arranged in a complex medium, acting synergistically. In many cases, they are stabilized by the mixture of components present in their natural environment [35]. However, after isolation, their activity may be reduced or even completely lost. In this sense, the use of jussara pulp integrally to produce NFs can be proposed to mitigate or prevent the loss of functionality of these compounds. The incorporation of bioactive compounds into nanocomposites, as well as the production of nanocarriers, can increase the action of these compounds, protect the substances, increase solubility, and allow more precise targeting of molecules in the body [35]. Experimental design plays a critical role in acquiring valid elucidations of results gathered from observational and empirical reports. Designing this work will allow to differentiate the effect of the variables of interest from those not pertinent and, hence, to obtain overall conclusions from the study [36].

As revealed by scarce literature in this subject, the development of nanostructures to include bioactive compounds using electrospinning technology has not yet been extensively studied. Thus, the work tackled precisely this matter, by establishing the conditions to assemble nanostructures using PEO and to incorporate bioactive compounds into core-shell NFs, as well as assessing microscopic and physical characteristics of the material produced. Jussara pulp was used herein to validate the method of incorporating bioactive compounds into the nanostructures and also as a rich source of anthocyanins.

2. Materials and Methods

2.1. Solutions Preparation for Electrospinning

Solutions used for the electrospinning process were prepared using PEO (900,000 g·mol⁻¹, Sigma Aldrich, St. Louis, MO, USA) concentrations ranging from 6% to 8% with and without NaCl (0–2.5%, *w/v*) in water. The samples were homogenized in a magnetic agitator at 25 °C.

2.2. Electrospinning Process

The polymeric structures were prepared using laboratory-scale electrospinning (FLUIDNATEK LE-10, BIOINICIA, Spain). The collector was a plate made of anodized aluminum. The samples were produced and collected at controlled room temperature (20 to 25 °C) and relative humidity (50% to 60%). The process and solution parameters most studied to the electrospinning (i.e., the feeding rate, the PEO concentration, NaCl concentration, the tip-to-collector distance (TCD), and the applied voltage) were varied. A thorough investigation was performed to find the optimum conditions of the process. The moisture of the electrospun samples was accepted to be removed entirely during the electrospinning process, so the results of all analyses were expressed on a dry weight basis.

2.3. Experimental Design

The effects of feeding rate, PEO concentration, NaCl concentration, tip-to-collector distance (TCD), and the applied voltage on nanostructures production were studied employing a 2^{5-1} fractional design with four central points, giving a total of 20 trials. The experiments of the 2^{5-1} fractional factorial design were carried out using three values for each of the independent variables (Table 1). For each method setup, the response of the experimental designs was the weight of samples collected (mg). An estimate of the main effect was obtained by evaluating the difference in process performance caused by a change from the low (−1) to the high (+1) levels of the corresponding variable. All the samples were obtained using the uniaxial electrospinning.

Table 1. Parameters (feeding rate, PEO concentration, NaCl concentration, tip-to-collector distance (TCD), and applied voltage) used to evaluate the production of electrospinning nanostructures in the fractional factorial design.

Samples	PEO (%) (w/v)	NaCl (%) (w/v)	TCD (cm)	Voltage (kV)	Feeding Rate ($\mu\text{-h}^{-1}$)	pH	Conductivity ($\mu\text{S}\cdot\text{cm}^{-1}$)	Zeta Potential (mV)
1	6.0	0.0	10.0	10.0	3000	8.76	171.8	−0.3
2	8.0	0.0	10.0	10.0	150	8.64	128.8	−0.3
3	6.0	2.5	10.0	10.0	150	8.26	27,500.0	−0.9
4	8.0	2.5	10.0	10.0	3000	8.37	23,900.0	−0.9
5	6.0	0.0	15.0	10.0	150	8.76	171.8	−0.3
6	8.0	0.0	15.0	10.0	3000	8.64	128.8	−0.3
7	6.0	2.5	15.0	10.0	3000	8.26	27,500.0	−0.9
8	8.0	2.5	15.0	10.0	150	8.37	23,900.0	−0.9
9	6.0	0.0	10.0	24.0	150	8.76	171.8	−0.3
10	8.0	0.0	10.0	24.0	3000	8.64	128.8	−0.3
11	6.0	2.5	10.0	24.0	3000	8.26	27,500.0	−0.9
12	8.0	2.5	10.0	24.0	150	8.37	23,900.0	−0.9
13	6.0	0.0	15.0	24.0	3000	8.76	171.8	−0.3
14	8.0	0.0	15.0	24.0	150	8.64	128.8	−0.3
15	6.0	2.5	15.0	24.0	150	8.26	27,500.0	−0.9
16	8.0	2.5	15.0	24.0	3000	8.37	23,900.0	−0.9
17	7.0	1.25	12.5	17.0	1575	8.39	16,680.0	−0.4
18	7.0	1.25	12.5	17.0	1575	8.39	16,680.0	−0.4
19	7.0	1.25	12.5	17.0	1575	8.39	16,680.0	−0.4
20	7.0	1.25	12.5	17.0	1575	8.39	16,680.0	−0.4

All materials were generated using uniaxial electrospinning.

2.4. Characterization of Solutions and Nanostructures

2.4.1. Determination of Solution Properties

The solutions were prepared according to the conditions presented (Table 1), and several determinations were achieved, including the conductivity, measured with a digital conductivimeter (Hanna HI 8733, Brazil); pH, measured with a pHmeter (Hanna HI5522, Brazil). Additionally, the optical properties of PEO solutions prepared using the polymer at different conditions were characterized

using Ultraviolet-visible absorption spectroscopy (UV-Vis). The zeta potential was measured by a dynamic light scattering instrument, a Zetasizer (Malvern Instruments, Malvern, UK) with an MPT-2 titrator. All the measurements were obtained from three independent assessments.

2.4.2. Characterization of Electrospun Samples

After the NFs samples were produced, using PEO or mixtures of PEO-NaCl, a characterization was performed. The characteristic fundamental vibrational modes and wavenumbers from experimental spectra were obtained using Fourier-transform infrared spectroscopy (FTIR) (Bruker Alpha-P, in the range $4000\text{--}500\text{ cm}^{-1}$). Complementary, to confirm the composition of the obtained structures observed in some of the characterization analyses, the samples were also mapped by Energy dispersive X-ray spectroscopy (EDX) performed by an FE-SEM Philip XL-30 TMP coupled to an Oxford EDS. The field emission scanning electron microscopy (FE-SEM Supra 35 VP- equipment, Carl Zeiss, Germany) was used to obtain the micrography images of the samples. To help expedite measurement in FE-SEM images and reduce bias from manual data processing, the tool DiameterJ (ImageJ program) was applied in the present work [37].

In addition, the contact angle of the electrospun samples was measured to determine surface hydrophobicity. The analysis was performed using a sessile drop method in a Rame-Hart goniometer (Model 260-F) coupled to the software DROPimage Next, using deionized water as wetting liquids, the droplet volume of each standard wetting liquid was determined to be $5\text{ }\mu\text{L}$. At room temperature ($26 \pm 1\text{ }^\circ\text{C}$), this was obtained at 10 random locations on the surface of the composites. From these measurements, we determined the mean and standard deviation.

2.5. Incorporation of Jussara Pulp as a Source of Anthocyanins

2.5.1. Solutions Preparation for Electrospinning

The feed solutions were prepared in acetate buffer (pH 4.5) with 6% PEO and 10% lyophilized jussara pulp (preliminary tests were accomplished to determine the best concentration of the jussara pulp to incorporate into the electrospun material). The jussara pulp used was acquired straight from producers associated with the Jussara Project from Ubatuba City–São Paulo–Brazil. The frozen jussara pulp was transported in coolers, lyophilized (to maintain the bioactive compounds intact), and stored in a freezer until the analysis. Jussara pulp was reconstituted and filtered before the electrospinning assays.

2.5.2. Electrospinning Process

The electrospinning process was conducted on the equipment (FLUIDNATEK LE-10, BIOINICIA, Spain) at room temperature to produce NFs containing jussara pulp. The collector was a plate made of anodized aluminum. The samples were prepared and collected at controlled room temperature ($20\text{--}25\text{ }^\circ\text{C}$) and relative humidity ($50\%\text{--}60\%$). The jussara pulp was successfully included using the electrospinning technique at both operational modes of the equipment, uniaxial and coaxial, to form core-shell NFs. The operational conditions for the electrospinning process in the uniaxial setup were: feeding rate of $150\text{ }\mu\text{L}\cdot\text{h}^{-1}$; TCD at 15 cm; applied voltage of 10 kV. The feeding solution presented a pH of 5.6, the same as the natural jussara pulp. While for the coaxial mode of operation, PEO%, TCD and applied voltage followed the same operational conditions of the uniaxial method. However, feeding rate was adapted to allow the setup of the equipment. Therefore, for a shell (polymeric solution), the flow rate was $400\text{ }\mu\text{L}\cdot\text{h}^{-1}$, whereas the core (jussara pulp) employed a flow rate of $200\text{ }\mu\text{L}\cdot\text{h}^{-1}$.

2.5.3. Characterization of Electrospun Samples

After the NFs containing jussara pulp samples were produced, characterization of the material was performed. Field emission scanning electron microscopy (FE-SEM Supra 35 VP- equipment, Carl Zeiss, Germany) was used to obtain the micrography images of the samples. To help expedite measurement

in FE-SEM images and reduce bias from manual data processing, the tool DiameterJ (ImageJ program) was applied [37]. Additionally, fundamental vibrational modes and wavenumbers from experimental spectra were obtained using Fourier-transform infrared spectroscopy (FTIR) (Bruker Alpha-P, in the range 4000–500 cm^{-1}).

2.6. Statistical Analysis

Measurements from the samples were carried out independently in triplicate and compared by applying analysis of variance (ANOVA) using the degree of significance of 95% ($p < 0.05$), followed by Tukey's post hoc test.

3. Results and Discussion

3.1. Electrospinning Process

Considering the factors detected by a careful literature search on parameters that could influence production of nanostructures using the electrospinning process, feeding rate (150–3000 $\mu\text{L}\cdot\text{h}^{-1}$, PEO concentration (1%–8% w/v), NaCl concentration (0%–2.5% w/v), tip-to-collector distance (TCD) (10–15 cm), and applied voltage (10–24 kV) featured among the main findings [22–25,38–42]. Unexpectedly, in contradiction to the results presented in the consulted literature, none of the assays performed using PEO concentrations under 6% formed any kind of polymeric structures and, in all cases, regardless of any other parameter adjustment within the aforementioned ranges, the solution would drop as it went through the TCD and contacted the collector.

Due to such discrepancy between the data found in the literature and these preliminary results, an alteration to the variation in PEO concentrations was applied. Instead of using the PEO concentration 1%–8% (w/v), the experiments applied 6%–8% (w/v) of PEO; all the conditions used are presented (Table 1). Composition of the PEO/NaCl solutions, as well as the other parameters assessed for nanostructures production and conductivity measurements, are shown in Table 1. It must be highlighted that PEO is widely used as a carrier due to its ability to dissolve a wide variety of salt and superb mechanical properties compared with those of other polymers.

3.2. Experimental Design

The assays from the experimental design matrix were randomly performed to produce electrospun structures (Table 1). In the present study, several operational challenges occurred regarding the electrospinning process for nanostructures production using the chosen parameters. The samples 1, 3, 4, 6, 10, 16, 17, 18, 19, and 20 were unsuccessful assays since it was not possible to obtain any kind of polymer fiber using the established conditions of those experiments. Still, we could not find a specific variable or combination thereof to explain this result, mainly due to the lack of data to evaluate the experimental design purposed. It appears that some kind of interactions between the variables assessed possesses an antagonist effect regarding the electrospun formation. Therefore, 10 samples (out of 20) could not be considered, and the experimental design was not fully explored herein.

The central points of any experimental design provide additional degrees of freedom for error estimation, which increases power when testing for statistical significance of effects [43–46]. In our work, the central points did not provide any electrospun samples (experiments 17–20) difficulting the statistical analysis over the remaining effective samples. On the other hand, from the conditions used to produce samples 2, 5, 7, 8, 9, 11, 12, 13, 14, and 15, it was possible to obtain different structures, showing very diverse formation between the samples.

3.3. Characterization of Solutions and Nanostructures

The conductivity values obtained for polymer solutions ranged from 128.8 to 27,500.0 $\mu\text{S}\cdot\text{cm}^{-1}$, and, as expected, the solutions containing higher amounts of NaCl presented higher conductivity. Samples lacking NaCl decreased their conductivity in proportion to PEO concentration, even with

the PEO not being electrically charged. The rise in conductivity values in the samples with a higher amount of salt can be attributed to an increase in the number of mobile ions as a result of salt concentration [47]. Several authors affirm that the presence of NaCl—besides increasing conductivity values and, consequently, interacting at the polymer-bulk medium interface between the hydrophilic polymer and water molecules—can impact the size of the obtained structure [22,40]. Therefore, especially considering the principle of the electrospinning process, it is an essential variable to study. The values for pH ranged from 8.26 to 8.76, showing a small range of variation (Table 1).

All electrospun samples had negative surface charges (Table 1), and their values ranged from -0.3 to -0.9 mV. The addition of NaCl decreased the zeta potential value. The negative lower values (or positive higher values) of zeta potential is an indication of stability [48]. From the obtained data regarding UV-vis absorption spectroscopy results (Figure S1), it is possible to affirm that the behavior of PEO solutions followed the same profile regardless of NaCl addition or concentration. According to the parameters of process variation, different structures in a distinct scale were obtained, showing a vast range of results (Figure 1).

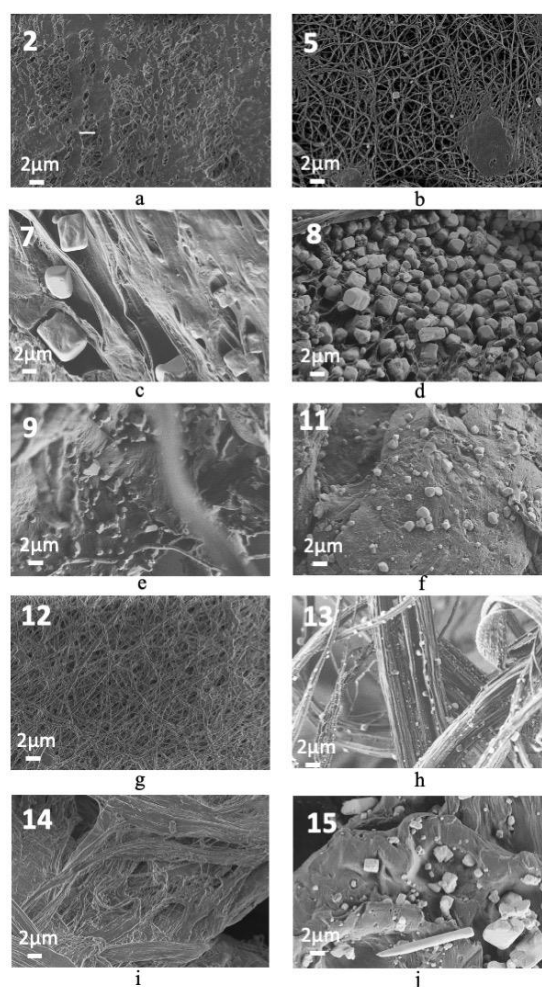


Figure 1. FE-SEM images of effective electrospun samples obtained from fractional factorial design samples: (a) sample 2, (b) sample 5, (c) sample 7, (d) sample 8, (e) samples 9, (f) sample 11, (g) sample 12, (h) samples 13, (i) sample 14, and (j) sample 15.

FE-SEM images (Figure 1) show that fibers were formed, creating unique shapes with a high number of porous structures, showing the most different formation possibly because the polymeric solution did not dry out before reaching the collector. The micrographs obtained for sample 8 (Figure 1d) show mostly NaCl crystals. Although some similarities are observed concerning the final product

obtained for samples 7 (Figure 1c), 9 (Figure 1e), 11 (Figure 1f) and 15 (Figure 1j), NFs were not formed. In turn, in samples 5 (Figure 1b), 12 (Figure 1g), 13 (Figure 1h) and 14 (Figure 1i), PEO presented NFs shape. The image representing sample 5 (Figure 1b) presents solution droplets on the fiber material. For samples 7 (Figure 1c) and 12 (Figure 1g) an excellent homogeneity of the obtained fibers was observed, while, for sample 13 (Figure 1h), larger fibers were obtained. The production of smaller fibers is preferred over larger fibers due to their greater surface area, which can maximize the properties of incorporated biocomposites.

The evaluated conditions yielded fibers with no preferential direction of orientation (Figure S2). In addition, data were obtained after the measurement of NFs diameters (Table 2).

Table 2. Diameter values (Mean \pm SD) (nm) from the resulting materials produced in samples 2, 5, 7, 8, 9, 11, 12, 13, 14, and 15 conditions of experimental design

Measurements (Samples)	Mean Diameter (nm)	Minimum Diameter (nm)	Maximum Diameter (nm)
2	525.16 ^{ab} \pm 120	119.7	1333.62
5	126.00 ^a \pm 50	52.22	199.50
7	5589.37 ^d \pm 659	3108.60	9442.59
8	2408.09 ^c \pm 980	1533.12	3871.30
9	2643.67 ^c \pm 666	1870.25	8195.25
11	29,957.27 ^e \pm 6032	3710.90	50,939.74
12	94.02 ^a \pm 32	51.50	177.94
13	906.35 ^b \pm 132	249.08	1618.59
14	484.88 ^{ab} \pm 98	72.46	1549.17
15	2577.16 ^c \pm 765	1381.50	4918.4

Different letters in the same column represent significantly different values ($p < 0.05$).

The diameters of NFs composed by PEO and jussara ranged from 94.02 ± 40.0 nm to $29,957.27 \pm 6032$ nm, and our aim was to select the solutions yielding materials with smaller measurements. An analysis of variance (ANOVA) using the degree of significance of 95% ($p < 0.05$), followed by Tukey's post hoc test was applied on the data to determine the statistical relations among the acquired samples. Comparing the diameters obtained, an immense variation is observed. On an individualized evaluation, samples 2, 5, 12, and 14 showed no difference ($p < 0.05$) regarding the size of the electrospun samples produced (Table 2). Even though, numerically, the samples appear very different among them, all four samples present adequate structure size for incorporation of the bioactive compound, thus exhibiting potential for the jussara pulp NFs production.

Comparing among the samples produced, some did not reveal statistical differences within one another (this is the case for samples 13, 2, and 14, as well as for samples 8, 9, and 15), whereas statistical differences were verified between samples 7 and 11. Samples 7, 8, 9, 11, 13, and 15 showed micro-sized structures, that is, they provide smaller surface area, thus turning their appeal for incorporation bioactive compounds less attractive.

Since maximization parameters for nanostructure production were not achieved from the experimental design applied herein, a more panoramic interpretation of the conditions studied could be provided by other analysis upon the differences observed among the conditions that successfully produced materials. In this context, our results seem to confirm our hypothesis, since the obtained materials present incontestable differences depending on the combination of the parameters applied to produce each sample.

To better understand the role of NaCl on the formed polymeric structure, FTIR analyses were performed (Figure 2). For this analysis, samples 5 and 12 were chosen. The chosen conditions were based on trials that yielded nanosized structures. The characteristic fundamental vibrational modes and wave numbers exhibited for these samples collected from the FTIR experimental spectra (Figure 2) are listed (Table 3) and are in agreement with data reported in the literature [49–54].

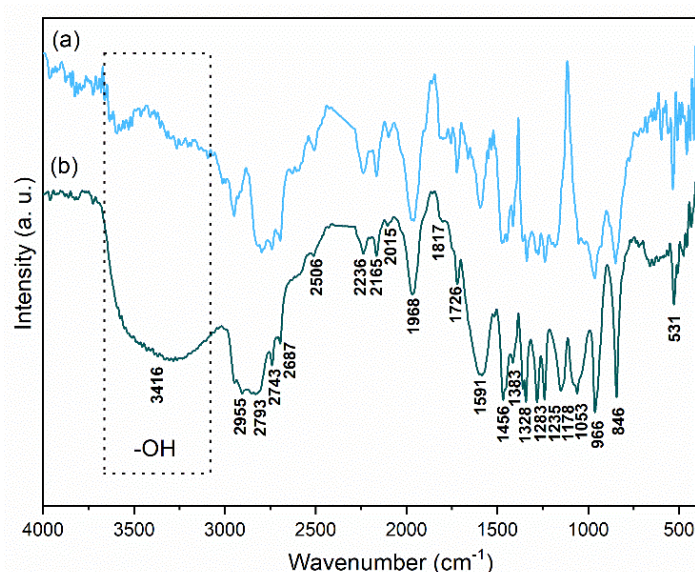


Figure 2. FTIR spectra from the conditions of experimental design resulting in the obtention of samples (a) 5 and (b) 12, at room temperature.

Table 3. Wavenumbers and assignments of IR bands exhibited by samples 5 and 12. Where, ν = stretch, δ = scissor/deformation, ω = wag, ρ = rock, τ = twist. The subscripts s and as refer to symmetric and asymmetric vibrational modes, respectively.

Wavenumber (cm ⁻¹)	Assignment
850	ρ (CH ₂) + δ (C-O-C)
960	ρ_{as} (CH ₂) + ν (CH ₂)
1052	ν (C-C) + ρ (CH ₂)
1150	ν_s (C-O-C)
1238, 1278	τ_s (CH ₂), τ_{as} (CH ₂)
1338, 1358	A doublet ω (CH ₂)
1445, 1471	δ_s (CH ₂), δ_{as} (CH ₂)
1722	ν (C=O)
2950–2700	ν_s (CH ₂), ν_{as} (CH ₂)

FTIR bands ranging from weak to medium intensities found in the spectra region 400 to 4000 cm⁻¹ for both evaluated conditions involve the coupling of several vibrational modes of the CH₂ group and the skeletal modes. These bands are relatively sensitive to chain conformation changes [51,55]. The absorbance peak in the 3416 cm⁻¹ regions can be the result of water absorbance [56]. As seen in the selected frame, it is more intense in the sample prepared with NaCl and can be attributed to the absorption of humidity from the air. Considering the polymer produced with the addition of NaCl, changes in the intensities and small displacements of the bands can be observed. However, no bands were suppressed, and no new bands were formed. This result suggests that the incorporation of NaCl in PEO solutions does not cause significant variations in its structure.

Furthermore, to investigate whether the factors varied on the present study changes the wettability of the nanostructures, the contact angle was used to evaluate the surface of NFs obtained from samples 2, 5, 7, and 14, since they presented no difference, statistically, in terms of diameter. The contact angle values were determined for electrospun samples (Figure 3) and the results ranged from 37.4° ± 3.3° to 57.7° ± 1.9°, showing no statistical difference ($p < 0.01$) between them. All contact angle values evaluated in water were lower than 90°, indicating that the samples possess a hydrophilic character regardless of the conditions applied to obtain the nanostructures. However, no difference was observed regarding the hydrophilicity.

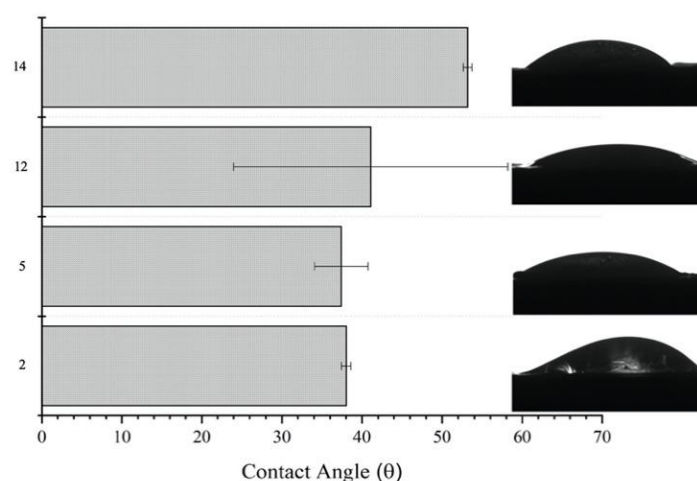


Figure 3. Contact angle values (Mean \pm SD) and images from the conditions of experimental design resulting in the obtention of samples 2, 5, 12, and 14.

Samples 5 and 12 were mapped using EDX to confirm the composition of the obtained structures observed (Figure 4a,b respectively). Within the boundaries of the NFs, a higher accumulation of counts for C and O were present, according to the element map. C and O of the map are due to the presence of these elements in PEO NFs. No presence of N in the PEO sample is observed, since it does not contain N in its composition. A small amount of Na and Cl is also found for sample 5 (Figure 4a), possibly due to salts present in the water used to make up PEO solutions. Regarding sample 12 (Figure 4b), a high distribution of Na and Cl is observed throughout the sample map, as expected.

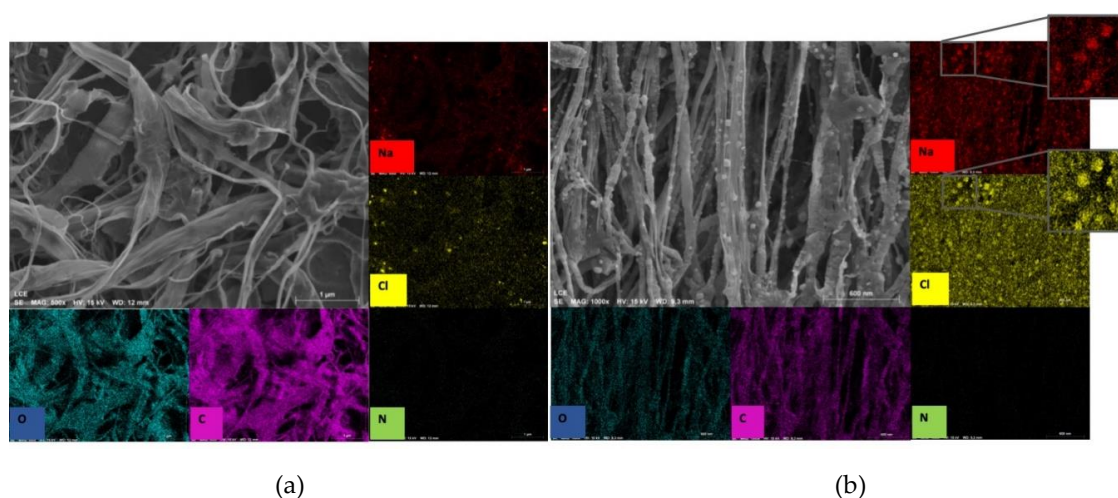


Figure 4. EDX map from the conditions of experimental design resulting in samples (a) 5 and (b) 12.

3.4. Incorporation of Jussara Pulp as a Source of Anthocyanins

Jussara pulp was used as a model to verify the success of the method to incorporate bioactive compounds, such as anthocyanins and other phenolics, into the produced structures using the electrospinning method, forming core-shell NFs. Therefore, the four conditions (samples 2, 5, 12, and 14) that presented no statistical difference among each other were used to compare the behavior of jussara addition. The parameters chosen for pulp incorporation are comparable those applied to sample 5 from the experimental design since, in this case, the lowest amount of polymer is used, representing an economical use of the resources.

FE-SEM images comparing fibers obtained either using only PEO or after the incorporation of core-shell NFs with jussara were evaluated (Figure 5). The structures produced with jussara pulp

show a heterogeneous format compared with NFs of PEO, in which a clean/beadles morphology was observed in some samples. Measurement in FE-SEM images was also obtained, and the mean core-shell NFs diameter was 129.5 ± 51.0 nm. In terms of fiber size, there was no statistical difference after jussara pulp incorporation, as mean fiber diameters were 126.5 ± 50.0 nm and 144.3 ± 86.1 nm for uniaxial and coaxial modes of operation, respectively, in samples without jussara. Smaller diameters of core-shell NFs results in higher surface area of the structure, thus maximizing bioavailability of the jussara pulp, which may then increase the antioxidant capacity of the final material.

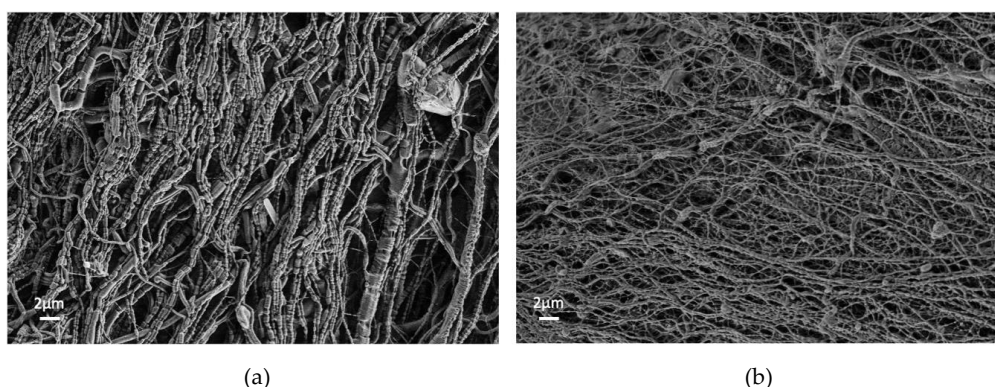


Figure 5. SEM images electrospun core-shell NFs samples collected from jussara pulp incorporation using the electrospinning technique applying both operation modes: (a) coaxial and (b) uniaxial.

FTIR spectra of sample 5 (PEO 6%) (6a), of the jussara pulp alone (6b), of a sample composed by PEO 6% and jussara (uniaxial electrospinning) (6c), and of a sample comprised by PEO 6% and jussara (coaxial electrospinning) (6d), at room temperature, are shown (Figure 6a–d). Characteristic bands of the structure of the anthocyanins can be observed in the FTIR spectrum of natural jussara pulp (Figure 6b). The anthocyanins exhibited absorption bands situated at 2923 cm^{-1} , which belong to the saturated hydrocarbon groups (corresponding to a methyl group (CH_3)); at 1749 cm^{-1} , fitting the stretching vibration of C–O; and at 1072 cm^{-1} , corresponding to bending vibration of C–O–C groups (indicating the presence of carbohydrates) [57]. Bands corresponding to the skeletal stretching vibration of the aromatic rings and =C–O–C group of flavonoids (1072 , 1506 , and 1271 cm^{-1}) were also visible [58]. The bands situated between 1400 and 1450 cm^{-1} are assigned to C–N vibration [58]. Besides, symmetrical and asymmetrical stretching vibration for the carboxyl ion (COO^-) indicating the existence of carboxylic acid, ester or carbonyl groups can also be observed at 1618 cm^{-1} [59,60].

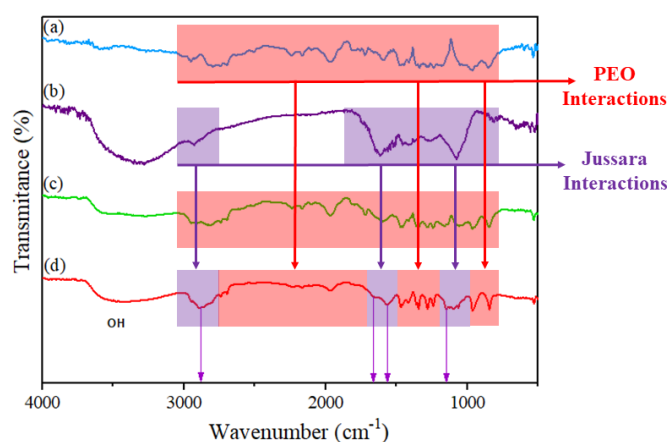


Figure 6. FTIR spectra: (a) sample 5 (PEO 6%), (b) jussara pulp, (c) sample composed by PEO 6% and jussara (uniaxial electrospinning), and (d) sample composed by PEO 6% and jussara (coaxial electrospinning), at room temperature.

FTIR spectra of core-shell NFs composed by PEO 6% and jussara (uniaxial electrospinning) (6c) and of a sample comprised of PEO 6% and jussara (coaxial electrospinning) (6d), are shown. Atomic interactions related to chemical bonding are considered an indication of compatibility between the polymer and the encapsulated bioactive product to produce a stable core-shell NF [61–64].

For both conditions, small displacements of the bands referring to the PEO were observed and can be interpreted as a result of the interaction between PEO and jussara pulp [5]. The distinct absorbance peak at the 3370 cm^{-1} regions can reflect water absorbance [56]. For the sample of PEO 6% and jussara 10% (uniaxial mode) (Figure 6c), the anthocyanin characteristic bands were not observed. This result could suggest that the jussara pulp may not be incorporated into the NFs; however other assays and additional analytical methods are necessary for confirmation.

Analyzing the spectrum (Figure 6d) for NFs composed by PEO 6% and jussara 10% (coaxial), an increase in intensity and resolution of the bands are observed, and, furthermore, the appearance of new bands is noted. Such features are suggestive of more substantial interactions between jussara and PEO by this method. New bands corresponding to anthocyanins situated at 1413 cm^{-1} (assigned to C–N vibration), at 1066 and 1091 cm^{-1} (corresponding to the skeletal stretching vibration of the aromatic rings and =C–O–C group of flavonoids), at 1655 cm^{-1} (symmetrical and asymmetrical stretching vibration for the carboxyl ion (COO[−])) and at 1780 cm^{-1} (stretching vibration of C–O) are visible.

Given the above considerations, it can be inferred that jussara pulp was successfully incorporated to the PEO NFs by the coaxial method. Still, more assessments should be made to complement the results generated in this study. Furthermore, it can also be concluded that the electrospinning method employed has a direct influence on the NFs containing jussara pulp.

The electrospinning close working system permits faster, safer and efficient production of NFs to be used in food stuff. Above all, dismissing specific solutions and used under ambient temperature. The two main configurations, uniaxial and coaxial, for use of the equipment were evaluated. Herein, the coaxial approach allowed the physical contact between jussara and PEO to occur more rapidly, preventing a possible intermolecular change and, thus maintaining the integrity of the structure of the anthocyanins. Coating material covers the encapsulated part, while the valuable compound is placed in the core portion. Indeed, control in the release step is best obtained by coaxial electrospinning procedure, even though the uniaxial electrospinning is considered a simpler process. Moreover, it is not possible to work with every polymer under uniaxial electrospinning [5,6].

The coaxial electrospinning procedure excludes the damaging results due to direct contact of the target compound with organic solvents or severe conditions during emulsification. The shell layer functions as a barrier to avoid the precipitate liberation of the water-soluble core contents. By changing the arrangement of the nanostructures, it is possible to modulate the release of the incorporated compounds accurately [48]. Therefore, our results agree with the consulted literature.

Jussara pulp incorporation into polymeric NFs enables the evaluations of likely uses of such material in food products, both as ingredients and as food coating, in which their beneficial properties could fully achieve their potential. Therefore, the results obtained represent a crucial step for the application of anthocyanins in food systems as natural pigments. Follow-up studies carried out in our research groups will use this data as a first step in the incorporation of nanostructures containing jussara pulp into foodstuff.

4. Conclusions

The development of structures from PEO solutions was obtained in a nanosized scale in some of the conditions evaluated. Our results seem to confirm our hypothesis since the obtained results present incontestable differences depending on the combination of the parameters applied in each assay tested. The nanostructures containing jussara pulp, a rich matrix for anthocyanins and other phenolics, using electrospinning technology, as well as characterization their properties, were also attained. Still, although electrospun nanostructures incorporated with jussara pulp was achieved, improvement of the applied variables is required to optimize the process as a whole, especially regarding the uniaxial

mode. Mainly, a decreased size in the NFs produced must be a requirement for bioactive compounds encapsulation. Further attempts at this matter must be conducted, allowing for enhanced incorporation of this natural pigment into food systems.

Supplementary Materials: The following are available online at <http://www.mdpi.com/2504-5377/4/2/14/s1>, Figure S1: UV-Vis spectral characteristics of the PEO and PEO + NaCl solutions; Figure S2: Analysis of SEM micrographs corresponding segmented images original SEM images are presented in Figure 5) by DiameterJ's Histogram algorithm and orientation degrees using OrientationJ, A: condition 1 (PEO 8%, without NaCl, TCD 10 cm, voltage 10 kV, feeding rate $150 \mu\text{-h}^{-1}$); B: condition 2 (PEO 6%, without NaCl, TCD 10 cm, voltage 24 kV, feeding rate $150 \mu\text{-h}^{-1}$); C: condition 3 (E and F) (PEO 6%, NaCl 2.5%, TCD 10 cm, voltage 24 kV, feeding rate $3000 \mu\text{-h}^{-1}$) and D: condition 4 (G and H) (PEO 8%, without NaCl, TCD 15 cm, voltage 24 kV, feeding rate $3000 \mu\text{-h}^{-1}$).

Author Contributions: Conceptualization, A.R.C.B.; methodology, S.d.P.R., M.A.G., J.T.D.M., R.d.S.P., M.A., and T.M.M.; formal analysis A.R.C.B.; investigation and writing—original draft preparation, S.d.P.R., M.A.G., J.T.D.M., R.d.S.P., V.V.D.R., A.C.L., M.B.E., M.A., T.M.M., E.L., and A.R.C.B.; writing—review and editing, A.R.C.B., A.C.L., M.B.E., T.M.M., E.L., V.V.D.R.; funding acquisition, A.R.C.B. and E.L. All authors have read and agreed to the published version of the manuscript.

Funding: This work was supported by the São Paulo Research Foundation (FAPESP) (process no. 2013/07296-2, 2018/01550-8; 2018/13408-1 and 2019/08975-7).

Acknowledgments: We acknowledge CAPES (001), FINEP, and CNPq for financial support. A sincere thank you to Paula Jimenez for her diligent proofreading of this article.

Conflicts of Interest: The authors declare no conflict of interest. The funders had no role in the design of the study; in the collection, analyses, or interpretation of data; in the writing of the manuscript, or in the decision to publish the results.

References

1. Kyselica, R.; Enikov, E.T.; Polyvas, P.; Anton, R. Electrostatic focusing of electrospun Polymer(PEO) nanofibers. *J. Electrostat.* **2018**, *94*, 21–29. [[CrossRef](#)]
2. Alehosseini, A.; Ghorani, B.; Sarabi-Jamab, M.; Tucker, N. Principles of electrospaying: A new approach in protection of bioactive compounds in foods. *Crit. Rev. Food Sci. Nutr.* **2018**, *58*, 2346–2363. [[CrossRef](#)] [[PubMed](#)]
3. Ramakrishna, S.; Fujihara, K.; Teo, W.-E.; Lim, T.-C.; Ma, Z. *An Introduction to Electrospinning and Nanofibers*; World Scientific: Singapore, 2005; ISBN 978-981-256-415-3.
4. Khajavi, R.; Abbasipour, M. Electrospinning as a versatile method for fabricating coreshell, hollow and porous nanofibers. *Sci. Iran.* **2012**, *19*, 2029–2034. [[CrossRef](#)]
5. Wen, P.; Zong, M.-H.; Linhardt, R.J.; Feng, K.; Wu, H. Electrospinning: A novel nano-encapsulation approach for bioactive compounds. *Trends Food Sci. Technol.* **2017**, *70*, 56–68. [[CrossRef](#)]
6. Jiang, H.; Wang, L.; Zhu, K. Coaxial electrospinning for encapsulation and controlled release of fragile water-soluble bioactive agents. *J. Control. Release* **2014**, *193*, 296–303. [[CrossRef](#)] [[PubMed](#)]
7. Morais, M.G.; Stillings, C.; Dersch, R.; Rudisile, M.; Pranke, P.; Costa, J.A.V.; Wendorff, J. Preparation of nanofibers containing the microalga *Spirulina* (Arthrospira). *Bioresour. Technol.* **2010**, *101*, 2872–2876. [[CrossRef](#)]
8. Wu, Y.H.; Yang, C.; Li, X.Y.; Zhu, J.Y.; Yu, D.G. Medicated Nanofibers Fabricated Using NaCl Solutions as Shell Fluids in Modified Coaxial Electrospinning. *J. Nanomater.* **2016**. [[CrossRef](#)]
9. Chayad, F.; Jabur, A.; Jalal, N. Effect of NaCl Solution Addition on Improving Some of the Physical Properties of Nylon 6 Solutions used for Electro Spinning Purpose. *Eng. Technol. J.* **2016**, *34*, 1265–1274.
10. Frenot, A.; Chronakis, I.S. Polymer nanofibers assembled by electrospinning. *Curr. Opin. Colloid Interface Sci.* **2003**, *8*, 64–75. [[CrossRef](#)]
11. Vroman, I.; Tighzert, L. Biodegradable polymers. *Materials (Basel)* **2009**, *2*, 307–344. [[CrossRef](#)]
12. Kai, D.; Liow, S.S.; Loh, X.J. Biodegradable polymers for electrospinning: Towards biomedical applications. *Mater. Sci. Eng. C* **2014**, *45*, 659–670. [[CrossRef](#)] [[PubMed](#)]
13. Khoo, H.E.; Azlan, A.; Tang, S.T.; Lim, S.M. Anthocyanidins and anthocyanins: Colored pigments as food, pharmaceutical ingredients, and the potential health benefits. *Food Nutr. Res.* **2017**, *61*, 1361779. [[CrossRef](#)] [[PubMed](#)]

14. Gordillo, B.; Sigurdson, G.T.; Lao, F.; González-Miret, M.L.; Heredia, F.J.; Giusti, M.M. Assessment of the color modulation and stability of naturally copigmented anthocyanin-grape colorants with different levels of purification. *Food Res. Int.* **2018**, *106*, 791–799. [[CrossRef](#)] [[PubMed](#)]
15. Braga, A.R.C.; Murador, D.C.; de Souza Mesquita, L.M.; de Rosso, V.V. Bioavailability of anthocyanins: Gaps in knowledge, challenges and future research. *J. Food Compos. Anal.* **2018**, *68*, 31–40. [[CrossRef](#)]
16. Domínguez-Hernández, C.R.; García-Alvarado, M.A.; García-Galindo, H.S.; Salgado-Cervantes, M.A.; Beristáin, C.I. Stability, antioxidant activity and bioavailability of nano-emulsified astaxanthin. *Rev. Mex. Ing. Quim.* **2016**, *15*, 457–468.
17. Gonçalves, R.F.S.; Martins, J.T.; Duarte, C.M.M.; Vicente, A.A.; Pinheiro, A.C. Advances in nutraceutical delivery systems: From formulation design for bioavailability enhancement to efficacy and safety evaluation. *Trends Food Sci. Technol.* **2018**, *78*, 270–291. [[CrossRef](#)]
18. Schulz, M.; Biluca, F.C.; Gonzaga, L.V.; da Borges, G.S.C.; Vitali, L.; Micke, G.A.; de Gois, J.S.; de Almeida, T.S.; Borges, D.L.G.; Miller, P.R.M.; et al. Bioaccessibility of bioactive compounds and antioxidant potential of juçara fruits (*Euterpe edulis Martius*) subjected to in vitro gastrointestinal digestion. *Food Chem.* **2017**, *228*, 447–454. [[CrossRef](#)]
19. Murador, D.C.; de Souza Mesquita, L.M.; Vannuchi, N.; Braga, A.R.C.; de Rosso, V.V. Bioavailability and biological effects of bioactive compounds extracted with natural deep eutectic solvents and ionic liquids: Advantages over conventional organic solvents. *Curr. Opin. Food Sci.* **2019**, *26*, 25–34. [[CrossRef](#)]
20. Braga, A.R.C.; da Figueira, F.S.; da Silveira, J.T.; de Moraes, M.G.; Costa, J.A.V.; Kalil, S.J. Improvement of Thermal Stability of C-Phycocyanin by Nanofiber and Preservative Agents. *J. Food Process. Preserv.* **2016**, *40*, 1264–1269. [[CrossRef](#)]
21. Duncan, T.V. Applications of nanotechnology in food packaging and food safety: Barrier materials, antimicrobials and sensors. *J. Colloid Interface Sci.* **2011**, *363*, 1–24. [[CrossRef](#)]
22. Da Figueira, F.S.; Gettens, J.G.; Costa, J.A.V.; de Moraes, M.G.; Moraes, C.C.; Kalil, S.J. Production of nanofibers containing the bioactive compound C-phycocyanin. *J. Nanosci. Nanotechnol.* **2015**, *16*, 1–8. [[CrossRef](#)] [[PubMed](#)]
23. Angammana, C.J.; Jayaram, S.H. Analysis of the Effects of Solution Conductivity on Electrospinning Process and Fiber Morphology. *IEEE Trans. Ind. Appl.* **2011**, *47*, 1109–1117. [[CrossRef](#)]
24. Kuntzler, S.G.; de Almeida, A.C.A.; Costa, J.A.V.; de Moraes, M.G. Polyhydroxybutyrate and phenolic compounds microalgae electrospun nanofibers: A novel nanomaterial with antibacterial activity. *Int. J. Biol. Macromol.* **2018**, *113*, 1008–1014. [[CrossRef](#)] [[PubMed](#)]
25. de Farias, B.S.; Vidal, É.M.; Ribeiro, N.T.; da Silveira, N.; da Silva Vaz, B.; Kuntzler, S.G.; de Moraes, M.G.; Cadaval, T.R.S.A.; de Almeida Pinto, L.A.; de Farias, B.S.; et al. Electrospun chitosan/poly(ethylene oxide) nanofibers applied for the removal of glycerol impurities from biodiesel production by biosorption. *J. Mol. Liq.* **2018**, *268*, 365–370. [[CrossRef](#)]
26. Abdel-Aal, E.-S.M.S.M.; Hucl, P.; Rabalski, I. Compositional and antioxidant properties of anthocyanin-rich products prepared from purple wheat. *Food Chem.* **2018**, *254*, 13–19. [[CrossRef](#)]
27. Braga, A.R.C.; de Mesquita, L.M.S.; Martins, P.L.G.; Habu, S.; de Rosso, V.V. Lactobacillus fermentation of jussara pulp leads to the enzymatic conversion of anthocyanins increasing antioxidant activity. *J. Food Compos. Anal.* **2018**, *69*, 162–170. [[CrossRef](#)]
28. Alberti, A.; Zielinski, A.A.F.; Couto, M.; Judacewski, P.; Mafra, L.I.; Nogueira, A. Distribution of phenolic compounds and antioxidant capacity in apples tissues during ripening. *J. Food Sci. Technol.* **2017**, *54*, 1511–1518. [[CrossRef](#)]
29. Murador, D.; Braga, A.R.; Da Cunha, D.; De Rosso, V. Alterations in phenolic compound levels and antioxidant activity in response to cooking technique effects: A meta-analytic investigation. *Crit. Rev. Food Sci. Nutr.* **2018**, *58*, 169–177. [[CrossRef](#)]
30. Jamar, G.; Santamarina, A.B.; Mennitti, L.V.; de Cássia Cesar, H.; Oyama, L.M.; de Rosso, V.V.; Pisani, L.P. Bifidobacterium spp. reshaping in the gut microbiota by low dose of juçara supplementation and hypothalamic insulin resistance in Wistar rats. *J. Funct. Foods* **2018**, *46*, 212–219. [[CrossRef](#)]
31. Santamarina, A.B.; Jamar, G.; Mennitti, L.V.; Ribeiro, D.A.; Cardoso, C.M.; De Rosso, V.V.; Oyama, L.M.; Pisani, L.P. Polyphenols-Rich Fruit (*Euterpe edulis Mart.*) Prevents Peripheral Inflammatory Pathway Activation by the Short-Term High-Fat Diet. *Molecules* **2019**, *24*, 1655. [[CrossRef](#)]

32. Oyama, L.M.; Silva, F.P.; Carnier, J.; de Miranda, D.A.; Santamarina, A.B.; Ribeiro, E.B.; Oller do Nascimento, C.M.; De Rosso, V.V. Juçara pulp supplementation improves glucose tolerance in mice. *Diabetol. Metab. Syndr.* **2016**, *8*, 8. [[CrossRef](#)] [[PubMed](#)]
33. Morais, C.A.; Oyama, L.M.; de Oliveira, J.L.; Garcia, M.C.; De Rosso, V.V.; Amigo, L.S.M.; do Nascimento, C.M.O.; Pisani, L.P. Jussara (*Euterpe edulis* Mart.) Supplementation during Pregnancy and Lactation Modulates the Gene and Protein Expression of Inflammation Biomarkers Induced by trans-Fatty Acids in the Colon of Offspring. *Mediators Inflamm.* **2014**, *2014*, 1–11. [[CrossRef](#)] [[PubMed](#)]
34. Da Silva, N.A.; Rodrigues, E.; Mercadante, A.Z.; De Rosso, V.V. Phenolic compounds and carotenoids from four fruits native from the Brazilian Atlantic forest. *J. Agric. Food Chem.* **2014**, *62*, 5072–5084. [[CrossRef](#)] [[PubMed](#)]
35. Giaconia, M.A.; dos Ramos, S.P.; Pereira, C.F.; Lemes, A.C.; De Rosso, V.V.; Braga, A.R. Cavalcante Overcoming restrictions of bioactive compounds biological effects in food using nanometer-sized structures. *Food Hydrocoll.* **2020**. In press. [[CrossRef](#)]
36. Moyaho, A.; Beristain-Castillo, E. Experimental Design: Basic Concepts. In *Encyclopedia of Animal Behavior*, 2nd ed.; Choe, J.C., Ed.; Academic Press: Oxford, UK, 2019; pp. 471–479. ISBN 978-0-12-813252-4.
37. Hotaling, N.A.; Bharti, K.; Kriel, H.; Simon, C.G., Jr. Diameter]: A validated open source nanofiber diameter measurement tool. *Biomaterials* **2015**, *61*, 327–338. [[CrossRef](#)]
38. Wu, D.; Wang, L.; Sun, D. Pattern deposition of electrosprayed polymer nanoparticles. In Proceedings of the 2007 7th IEEE Conference on Nanotechnology (IEEE NANO), Hong Kong, China, 2–5 August 2007; pp. 271–274.
39. Morota, K.; Matsumoto, H.; Mizukoshi, T.; Konosu, Y.; Minagawa, M.; Tanioka, A.; Yamagata, Y.; Inoue, K. Poly(ethylene oxide) thin films produced by electrospray deposition: Morphology control and additive effects of alcohols on nanostructure. *J. Colloid Interface Sci.* **2004**, *279*, 484–492. [[CrossRef](#)] [[PubMed](#)]
40. Schmatz, D.A.; Costa, J.A.V.; de Morais, M.G. A novel nanocomposite for food packaging developed by electrospinning and electrospaying. *Food Packag. Shelf Life* **2019**, *20*, 100314. [[CrossRef](#)]
41. Seo, H.B.; Kim, S.S.; Lee, H.Y.; Jung, K.H. High-level Production of Ethanol during Fed-batch Ethanol Fermentation with a Controlled Aeration Rate and Non-sterile Glucose Powder Feeding of *Saccharomyces cerevisiae*. *Biotechnol. Bioprocess Eng.* **2009**, *14*, 591–598. [[CrossRef](#)]
42. Da Vaz, B.S.; da Mastrantonio, D.J.S.; Costa, J.A.V.; de Morais, M.G.; de Morais, M.G. Green alga cultivation with nanofibers as physical adsorbents of carbon dioxide: Evaluation of gas biofixation and macromolecule production. *Bioresour. Technol.* **2019**, *287*, 121406. [[CrossRef](#)]
43. Alves, F.G.; Mauger, F.; Burkert, J.F.M.; Kalil, S.J. Maximization of b-galactosidase production: A simultaneous investigation of agitation and aeration effects. *Appl. Biochem. Biotechnol.* **2010**, *160*, 1528–1539. [[CrossRef](#)]
44. Braga, A.R.C.; Gomes, P.A.; Kalil, S.J. Formulation of Culture Medium with Agroindustrial Waste for β -Galactosidase Production from *Kluyveromyces marxianus* ATCC 16045. *Food Bioprocess Technol.* **2012**, *5*, 1653–1663. [[CrossRef](#)]
45. Machado, J.R.; Behling, M.B.; Braga, A.R.C.; Kalil, S.J. β -Galactosidase production using glycerol and byproducts: Whey and residual glycerin. *Biocatal. Biotransform.* **2015**, *33*, 208–215. [[CrossRef](#)]
46. Braga, A.R.C.; Silva, M.F.; Vladimir Oliveira, J.; Treichel, H.; Kalil, S.J. Effect of compressed fluids treatment on β -galactosidase activity and stability. *Bioprocess Biosyst. Eng.* **2012**, *35*, 1541–1547. [[CrossRef](#)] [[PubMed](#)]
47. Gondaliya, N.; Kanchan, D.K.; Sharma, P.; Joge, P. Structural and conductivity studies of poly (ethylene oxide)–silver triflate polymer electrolyte system. *Mater. Sci. Appl.* **2011**, *2*, 1639. [[CrossRef](#)]
48. Isik, B.S.; Altay, F.; Capanoglu, E. The uniaxial and coaxial encapsulations of sour cherry (*Prunus cerasus* L.) concentrate by electrospinning and their in vitro bioaccessibility. *Food Chem.* **2018**, *265*, 260–273. [[CrossRef](#)]
49. Chen, H.; Jiang, C.; Wu, H.; Chang, F. Hydrogen bonding effect on the poly (ethylene oxide), phenolic resin, and lithium perchlorate–based solid-state electrolyte. *J. Appl. Polym. Sci.* **2004**, *91*, 1207–1216. [[CrossRef](#)]
50. Hoffmann, C.L.; Rabolt, J.F. Self-assembled thin-film blends by polymer codeposition: Poly (ethylene oxide) and poly (methyl methacrylate). *Macromolecules* **1996**, *29*, 2543–2547. [[CrossRef](#)]
51. Li, X.; Hsu, S.L. An analysis of the crystallization behavior of poly (ethylene oxide)/poly (methyl methacrylate) blends by spectroscopic and calorimetric techniques. *J. Polym. Sci. Polym. Phys. Ed.* **1984**, *22*, 1331–1342. [[CrossRef](#)]

52. Rajendran, S.; Kannan, R.; Mahendran, O. Ionic conductivity studies in poly (methylmethacrylate)–polyethylene oxide hybrid polymer electrolytes with lithium salts. *J. Power Sources* **2001**, *96*, 406–410. [[CrossRef](#)]
53. Xu, Y.; Zou, L.; Lu, H.; Kang, T. Effect of different solvent systems on PHBV/PEO electrospun fibers. *RSC Adv.* **2017**, *7*, 4000–4010. [[CrossRef](#)]
54. Yoshihara, T.; Tadokoro, H.; Murahashi, S. Normal Vibrations of the Polymer Molecules of Helical Conformation. IV. Polyethylene Oxide and Polyethylene-d 4 Oxide. *J. Chem. Phys.* **1964**, *41*, 2902–2911. [[CrossRef](#)]
55. Yokoyama, M.; Ishihara, H.; Iwamoto, R.; Tadokoro, H. Structure of poly (ethylene oxide) complexes. III. Poly (ethylene oxide)-mercuric chloride complex. Type II. *Macromolecules* **1969**, *2*, 184–192. [[CrossRef](#)]
56. Agatonovic-Kustrin, S.; Morton, D.W.; Yusof, A.P.M. The use of Fourier transform infrared (FTIR) spectroscopy and artificial neural networks (ANNs) to assess wine quality. *Mod. Chem. Appl.* **2013**. [[CrossRef](#)]
57. Vasincu, A.; Paulsen, B.; Diallo, D.; Vasincu, I.; Aprotosoai, A.; Bild, V.; Charalambous, C.; Constantinou, A.; Miron, A.; Gavrilescu, C. Vernonia kotschyana roots: Therapeutic potential via antioxidant activity. *Molecules* **2014**, *19*, 19114–19136. [[CrossRef](#)] [[PubMed](#)]
58. Favaro, L.I.L.; Balcão, V.M.; Rocha, L.K.H.; Silva, E.C.; Oliveira, J.M., Jr.; Vila, M.M.D.C.; Tubino, M. Physicochemical characterization of a crude anthocyanin extract from the fruits of jussara (*Euterpe edulis* Martius): Potential for food and pharmaceutical applications. *J. Braz. Chem. Soc.* **2018**, *29*, 2072–2088. [[CrossRef](#)]
59. Chang, H.; Kao, M.-J.; Chen, T.-L.; Chen, C.-H.; Cho, K.-C.; Lai, X.-R. Characterization of natural dye extracted from wormwood and purple cabbage for dye-sensitized solar cells. *Int. J. Photoenergy* **2013**, *2013*. [[CrossRef](#)]
60. Muchuweti, M.; Chikwambi, Z. Isolation and identification of anthocyanins in the fruit peels of starkrimson and marx red bartlett common pear cultivars and their bud mutants. *Am. J. Food Technol.* **2008**, *3*, 1–12. [[CrossRef](#)]
61. Vashisth, P.; Sharma, M.; Nikhil, K.; Singh, H.; Panwar, R.; Pruthi, P.A.; Pruthi, V. Antiproliferative activity of ferulic acid-encapsulated electrospun PLGA/PEO nanofibers against MCF-7 human breast carcinoma cells. *3 Biotech* **2015**, *5*, 303–315. [[CrossRef](#)]
62. Pezeshki, A.; Ghanbarzadeh, B.; Mohammadi, M.; Fathollahi, I.; Hamishehkar, H. Encapsulation of vitamin A palmitate in nanostructured lipid carrier (NLC)-effect of surfactant concentration on the formulation properties. *Adv. Pharm. Bull.* **2014**, *4*, 563–568.
63. Li, Y.; Yang, H.; Cao, F.; Zhao, X.; Wang, J. The stability of C-phycoerythrin doped silica biomaterials in UV irradiation. *J. Wuhan Univ. Technol. Sci. Ed.* **2009**, *24*, 852. [[CrossRef](#)]
64. Tamjidi, F.; Shahedi, M.; Varshosaz, J.; Nasirpour, A. Nanostructured lipid carriers (NLC): A potential delivery system for bioactive food molecules. *Innov. Food Sci. Emerg. Technol.* **2013**, *19*, 29–43. [[CrossRef](#)]

